

New Iron(III) Bis(acetylide) Compounds Based on the Iron Cyclam Motif

Zhi Cao, William P. Forrest, Yang Gao, Phillip E. Fanwick, Yang Zhang, and Tong Ren*

Department of Chemistry, Purdue University, West Lafayette, Indiana 47907, United States

Supporting Information

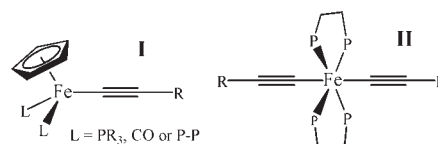
ABSTRACT: New *trans*-[Fe(cyclam)(C≡CR)₂]OTf compounds **2a/2b** [cyclam = 1,4,8,11-tetraazacyclotetradecane, R = Si^tPr₃ (**a**) or Ph (**b**), and OTf = trifluoromethanesulfonate] were prepared from the reaction between *trans*-[Fe(cyclam)-(OTf)₂]OTf (**1**) and LiC≡CR. The *trans* arrangement of the acetylide ligands in **2** was established from the X-ray diffraction study of **2a**, and the density functional theory calculations revealed significant $d\pi-\pi(C\equiv C)$ interactions.

Transition-metal acetylide compounds have received intense interest as potential molecular wires and other electronic and optoelectronic materials since the pioneering work on the linear [M]-acetylide polymers by Nast and Hagihara.¹ Facile charge transfer along the [M](C≡C)_m- linkage has been demonstrated for a number of metal centers in both bulk solution studies^{2,3} and nanojunction measurements.⁴ Many inspiring examples of iron monoacetylide compounds as molecular wires have been reported by the laboratories of Lapinte and Akita,⁵ where the piano-stool-type Fe^{II} centers, either CpFe(P-P)- or CpFe(CO)₂-, are prevalent (type I in Chart 1). In comparison, the iron bis(acetylide) compounds, developed mostly by the laboratory of Field, are rare and limited to Fe^{II} centers with acetylides in a *trans* geometry and bidentate chelating phosphines as the auxiliary ligands (type II in Chart 1).⁶

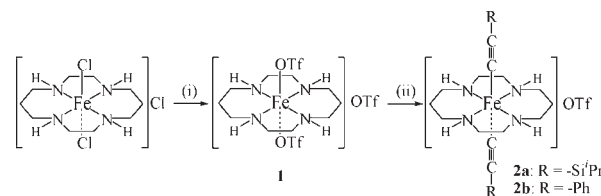
During the past decade, efforts from our and other laboratories have led to an extensive array of diruthenium acetylide compounds and a demonstration of the electronic delocalization therein.⁷ While the development of diruthenium compounds containing exotic acetylide ligands such as geminal diethynyl-ethenes remains a priority for us,⁸ we are vigorously seeking novel structural motifs that would also favor the *trans* arrangement of two acetylides. Of particular interest to us is the report of a series of chromium(III) cyclam bis(arylacetylides) by Wagenknecht et al., where the acetylide ligands adopt a *trans*-coordination geometry.⁹ Reported in this contribution are the preparation of iron(III) cyclam bis(acetylide) complexes (**2a** and **2b** in Scheme 1) and the elucidation of their electronic structures.

As shown in Scheme 1, the synthesis of bis(acetylide) compounds was preceded by the preparation of *trans*-[Fe(cyclam)(OTf)₂]OTf (**1**) from the reaction between trifluoromethanesulfonic acid (CF₃SO₃H) and known compound *cis*-[Fe(cyclam)Cl₂]Cl.¹⁰ The reaction between compound **1** and 4 equiv of LiC≡CR resulted in *trans*-[Fe(cyclam)(C≡CR)₂]OTf as a dark-orange powder for R as Si^tPr₃ (**2a**, 72%) and a dark-purple powder for R as Ph (**2b**, 64%), respectively. The *trans*-triflate compound **1** has a room temperature effective magnetic moment of 5.32 μ_B

Chart 1. Common Iron Acetylide Structures



Scheme 1. Synthesis of Iron(III) Cyclam Bis(acetylide) Complexes



Conditions: (i) CF₃SO₃H (excess), 40 h, room temperature; (ii) 4 equiv of LiC₂R, THF, 1 h.

(theoretical value for $S = 5/2$: 5.92 μ_B), indicating that the Fe^{III} center is high spin. On the other hand, the room temperature effective moments of compounds **2a** and **2b** are 1.94 and 1.89 μ_B, respectively, which are consistent with a $S = 1/2$ low-spin Fe^{III} center. Additionally, these compounds have been further characterized with UV-vis, HR-nESI-MS, and electrochemical techniques. The synthetic details and data for compounds **1** and **2** are provided in the Supporting Information.

The molecular structure of **2a** was determined by single-crystal X-ray diffraction. The asymmetric unit of crystal **2a** contains the halves of two independent cations. The structural plot and metric parameters of one of them are presented here, while the complete listing is given in the Supporting Information. It is clear from Figure 1 that the coordination sphere around the Fe^{III} center is pseudooctahedral with the C1-Fe1-C1A vector approximately orthogonal to the plane defined by the four N centers. The Fe-C bond length in **2a** [1.961(3) Å] is fairly close to the Fe^{II}-C bond lengths determined for *trans*-Fe(P-P)₂(C≡CR)₂-type compounds (1.92–1.97 Å).⁶

The redox activity of compounds **2a/2b** has been examined carefully using both cyclic voltammetric (CV) and differential pulse voltammetric (DPV) techniques. The CVs recorded are shown in Figure 2, while the DPVs are provided in Figure S2.

Received: April 24, 2011

Published: July 18, 2011

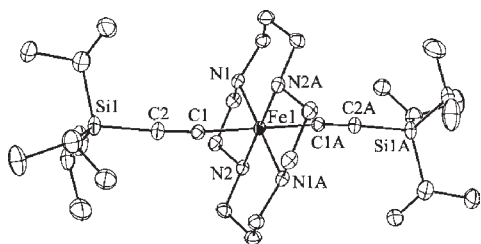


Figure 1. ORTEP plot of $2a^+$ at the 30% probability level. The triflate anion and H atoms were omitted for clarity. Selected bond lengths (Å) and angles (deg): Fe1–C1, 1.961(3); C1–C2, 1.210(4); Fe1–N1, 2.013(2); Fe1–N2, 2.007(2); C1–Fe1–N1, 91.63(11); C1–Fe1–N2, 89.69(11); N1–Fe1–N2, 94.57(9).

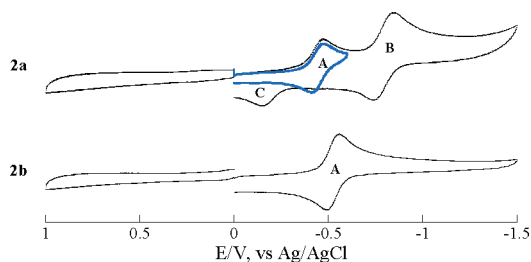


Figure 2. CVs recorded for compounds **2a** and **2b** in a 0.20 M THF solution of Bu_4NPF_6 . The inset in the CV of **2a** is the cathodic scan up to -0.6 V with the current scaled by a factor of 0.85 for clarity.

There is no detectable oxidation couple up to $+1.0$ V for both compounds **2a** and **2b**, which reflect the electron deficiency of the Fe^{III} species. Both compounds undergo a reversible $1e^-$ reduction (A), which is attributed to the reduction of Fe^{III} to Fe^{II} . The formal potential of **2b** is cathodically shifted from that of **2a**, indicating that the Fe^{III} center is substantially stabilized by an extended delocalization involving both phenyl rings. Interestingly, the reversible reduction A in **2a**, shown as an inset in Figure 2, becomes irreversible when the cathodic sweep is extended beyond -1.0 V, and a second reduction B is observed. Such behavior can be explained by an electrochemical–chemical–electrochemical (ECE) mechanism shown in Scheme 2: one of the $C\equiv CSi^iPr_3$ ligands in **2a** dissociates under more cathodic bias to yield a new species $2a''$, which undergoes the second reduction reversibly. The oxidation of $2a''$ on the return sweep results in peak C. Previously, Field et al. examined the redox activity of $trans\text{-}Fe(DMPE)(C\equiv CPh)_2$ [DMPE = bis(dimethylphosphine)ethane] and found two consecutive $1e^-$ oxidation couples, $Fe^{III/II}$ and $Fe^{IV/III}$, at $+0.01$ and 0.99 V in THF versus SCE.¹¹ In comparison, the $Fe^{III/II}$ couple in **2b** appears at -0.525 V versus Ag/AgCl, which is about 0.57 V more cathodic (after the correction for reference electrodes) than that of $Fe(DMPE)(C\equiv CPh)_2$. This clearly demonstrates that the Fe center can be selectively stabilized at formal oxidation state II or III by employing soft (P) or hard (N) auxiliary ligands, respectively.

The UV–vis absorption spectra of compounds **1** and **2a/2b** display rich features (Figure 3). Compound **1** has a very broad low-intensity absorption between 400 and 500 nm due to $d-d$ transitions and an intense band at 334 nm due to ligand-to-metal charge transfer (OTf to Fe^{III}). More intriguingly, both compounds **2a** and **2b** display highly structured bands in the visible region: namely, those at 370 , 410 , 430 , and 470 nm for **2a** and at 407 , 443 , 501 , and 555 nm for **2b**. Initially, it was

Scheme 2. Assignments of Reductions in Compound **2** Based on the ECE Mechanism

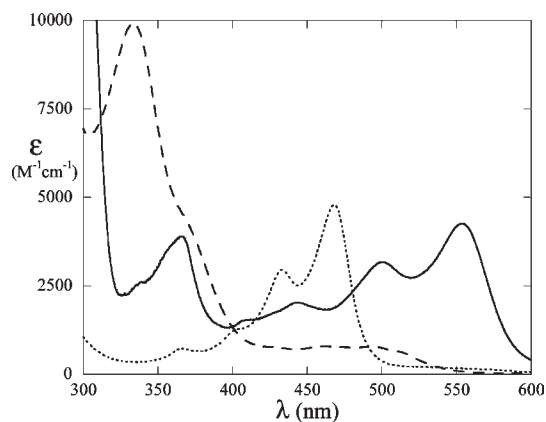
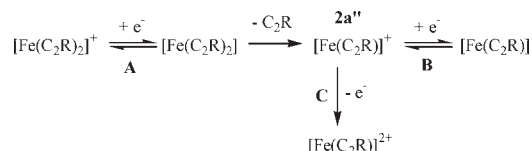


Figure 3. Absorption spectra of compounds **1** (dashed), **2a** (solid), and **2b** (dotted) recorded in acetonitrile.

suspected that the weaker bands were the vibronic sidebands of the most intense band (470 nm for **2a** and 555 nm for **2b**). However, a closer examination of the spectra plotted versus the wavenumber (Figure S3) revealed a large variation in the energy spacing between bands, which precludes the vibronic coupling interpretation. Nevertheless, a plausible assignment of the transitions can be achieved using the strong field limit of the Tanabe–Sugano diagram for a d^5 configuration:¹² the spin-allowed excitations from the ${}^2T_{2g}$ ground state to ${}^2T_{1g}$, ${}^2A_{2g}$, 2E_g , and ${}^2A_{1g}$ excited states results in peaks at $470/550$, $430/501$, $410/443$, and $370/407$ nm in **2a/2b**, respectively. Highly structured $d-d$ transitions were also observed for a series of aryethynyl $trans\text{-}[Cr(\text{cyclam})(C\equiv CAR)_2]^+$ (Ar = C_6H_5 , C_7H_7 , and $C_7H_4F_3$), albeit with extinction coefficients about an order of magnitude smaller than those of compounds **2a/2b**.⁹ As discussed in the density functional theory (DFT) section below, strong $Fe-C\equiv C$ π interactions are prevalent in **2a/2b**, which enables high molar absorption coefficients through intensity stealing.

Compounds **2a** and **2b** are quite different from the previously studied iron bis(acetylide) compounds⁶ in both the oxidation state (III vs II) and the auxiliary ligands (cyclam vs bidentate phosphines). Yet, the unusually intense $d-d$ transitions observed for both **2a** and **2b** imply significant $d\pi(Fe)-\pi(C\equiv C)$ interactions that typify the $CpFeL_2(C\equiv CR)$ -type compounds.² These observations prompted us to examine the electronic structure of type **2** compounds using the spin-unrestricted DFT calculations at the B3LYP/BP86/LanL2DZ level (Gaussian03 program).¹³ The calculations were based on the model cations $2a^{+/+}/2b^{+/+}$. The model cation $2a^{+/+}$ was optimized based on the crystal structure of $2a^+$ without truncation, and $2b^{+/+}$ was optimized from $2a^{+/+}$, with Si^iPr_3 groups being replaced by Ph groups. The most relevant valence molecular orbitals (MOs) are provided in Figure 4, while a detailed listing of the optimized

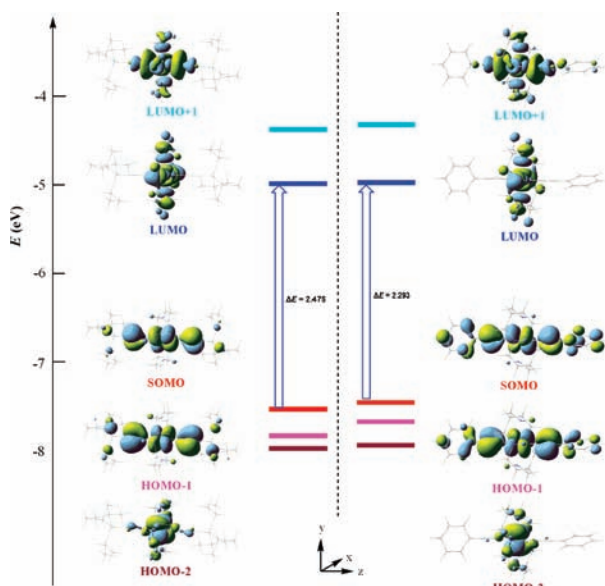


Figure 4. MO diagram for model compounds $2a'^+$ (left) and $2b'^+$ (right) based on α -spin orbitals (MO levels of β spin are shown in Figure S6 in the Supporting Information). The directions pointing toward the N atoms of the cyclam ring are designated as the X and Y axes.

geometries and MOs are given in the Supporting Information (Figures S4–S6 and Tables S1–S4).

The DFT results of $2a'^+$ and $2b'^+$ are in agreement with the ligand field theory prediction for a d^5 center in a strong field: an empty e_g set as the lowest unoccupied MO (LUMO; $d_{x^2-y^2}$) and LUMO+1 (d_{z^2}) and an occupied t_{2g} set as highest occupied MO (HOMO)–2, HOMO–1, and singly occupied MO (SOMO). The loss of orbital degeneracy is caused by both the low symmetry of the cyclam ligand (C_2 only) and the Jahn–Teller instability (in both O_h and D_{4h} settings). The two HOMOs, namely, HOMO–1 and SOMO, consist of the antibonding combinations of $d\pi$ and $\pi(C\equiv C)$, and the contribution from the latter is very significant. Similar interactions were noted for the piano-stool-type iron(III) monoacetylide compounds by Paul et al.¹⁴ The computed SOMO–LUMO gaps are qualitatively agreeable to the d–d transition optical gaps for **2a** (470 nm or 2.64 eV) and **2b** (550 nm or 2.25 eV). The SOMO and HOMO–1 of $2b'^+$ are of higher energy in comparison to those of $2a'^+$ because of stronger antibonding character through the introduction of phenyl groups. On the other hand, the LUMO levels of both $2a'^+$ and $2b'^+$ are approximately the same because of the absence of the contribution from the acetylide ligands. The reduction of the SOMO–LUMO optical gap in compound **2b** should be attributed to destabilization of the occupied $d\pi$ orbital(s). In addition, the pronounced $\pi(C\equiv C)$ contributions to both SOMO and HOMO–1 offer the possibility of intensity “stealing” in d–d bands.

In conclusion, we offered the first examples of iron(III) bis(acetylide) compounds **2a/2b** based on a iron cyclam synthon (**1**). Strong π interactions between the occupied $d\pi$ and $\pi(C\equiv C)$ orbitals are evident from both the absorption spectra and DFT calculations. Further syntheses of type **2** derivative compounds with donor/acceptor-substituted alkynes, isolation of their $1e^-$ reduction derivative (Fe^{II}), and the photophysical properties of these unique species are being investigated in our laboratory.

ASSOCIATED CONTENT

S Supporting Information. Synthesis and characterization of compounds **1**, **2a**, and **2b**, DFT calculations for model compounds $2a'$ and $2b'$, and an X-ray crystallographic file in CIF format for the structure determination of compound **2a**. This material is available free of charge via the Internet at <http://pubs.acs.org>.

AUTHOR INFORMATION

Corresponding Author

*E-mail: tren@purdue.edu.

ACKNOWLEDGMENT

We gratefully acknowledge financial support from the National Science Foundation (Grant CHE 1057621) and Purdue University.

REFERENCES

- (1) Nast, R. *Coord. Chem. Rev.* **1982**, *47*, 89. Hagihara, N.; Sonogashira, K.; Takahashi, S. *Adv. Polym. Sci.* **1981**, *41*, 149.
- (2) Paul, F.; Lapinte, C. *Coord. Chem. Rev.* **1998**, *178–180*, 431. Akita, M.; Koike, T. *Dalton Trans.* **2008**, 3523.
- (3) Szafert, S.; Gladysz, J. A. *Chem. Rev.* **2006**, *106*, 1. Yam, V. W. W.; Lo, K. K. W.; Wong, K. M. C. *J. Organomet. Chem.* **1999**, *578*, 3. Yam, V. W. W. *Acc. Chem. Res.* **2002**, *35*, 555. Ren, T. *Organometallics* **2005**, *24*, 4854.
- (4) Schull, T. L.; Kushmerick, J. G.; Patterson, C. H.; George, C.; Moore, M. H.; Pollack, S. K.; Shashidhar, R. *J. Am. Chem. Soc.* **2003**, *125*, 3202. Blum, A. S.; Ren, T.; Parish, D. A.; Trammell, S. A.; Moore, M. H.; Kushmerick, J. G.; Xu, G.-L.; Deschamps, J. R.; Pollack, S. K.; Shashidhar, R. *J. Am. Chem. Soc.* **2005**, *127*, 10010. Mahapatro, A. K.; Ying, J.; Ren, T.; Janes, D. B. *Nano Lett.* **2008**, *8*, 2131. Lu, Y.; Quardokus, R.; Lent, C. S.; Justaud, F.; Lapinte, C.; Kandel, S. A. *J. Am. Chem. Soc.* **2010**, *132*, 13519.
- (5) Lapinte, C. *J. Organomet. Chem.* **2008**, *693*, 793. Akita, M.; Moro-oka, Y. *Bull. Chem. Soc. Jpn.* **1995**, *68*, 420.
- (6) Field, L. D.; George, A. V.; Hambley, T. W. *Inorg. Chem.* **1990**, *29*, 4565. Field, L. D.; George, A. V.; Hambley, T. W.; Malouf, E. Y.; Young, D. J. *J. Chem. Soc., Chem. Commun.* **1990**, 931. Field, L. D.; George, A. V.; Malouf, E. Y.; Slip, I. H.; Hambley, T. W. *Organometallics* **1991**, *10*, 3842. Field, L. D.; Turnbull, A. J.; Turner, P. *J. Am. Chem. Soc.* **2002**, *124*, 3692. Field, L. D.; Magill, A. M.; Pike, S. R.; Turnbull, A. J.; Dalgarno, S. J.; Turner, P.; Willis, A. C. *Eur. J. Inorg. Chem.* **2010**, 2406.
- (7) Ren, T.; Zou, G.; Alvarez, J. C. *Chem. Commun.* **2000**, 1197. Wong, K.-T.; Lehn, J.-M.; Peng, S.-M.; Lee, G.-H. *Chem. Commun.* **2000**, 2259. Xu, G.-L.; Zou, G.; Ni, Y.-H.; DeRosa, M. C.; Crutchley, R. J.; Ren, T. *J. Am. Chem. Soc.* **2003**, *125*, 10057. Xu, G.-L.; Crutchley, R. J.; DeRosa, M. C.; Pan, Q.-J.; Zhang, H.-X.; Wang, X.; Ren, T. *J. Am. Chem. Soc.* **2005**, *127*, 13354. Ying, J.-W.; Liu, I. P.-C.; Xi, B.; Song, Y.; Campana, C.; Zuo, J.-L.; Ren, T. *Angew. Chem., Int. Ed.* **2010**, *49*, 954.
- (8) Forrest, W. P.; Cao, Z.; Fanwick, P. E.; Hassell, K. M.; Ren, T. *Organometallics* **2011**, *30*, 2075. Cao, Z.; Ren, T. *Organometallics* **2011**, *30*, 245.
- (9) Grisenti, D. L.; Thomas, W. W.; Turlington, C. R.; Newsom, M. D.; Priedemann, C. J.; VanDerveer, D. G.; Wagenknecht, P. S. *Inorg. Chem.* **2008**, *47*, 11452.
- (10) Chan, P. K.; Poon, C. K. *J. Chem. Soc., Dalton Trans.* **1976**, 858.
- (11) Field, L. D.; George, A. V.; Laschi, F.; Malouf, E. Y.; Zanello, P. *J. Organomet. Chem.* **1992**, *435*, 347.
- (12) Figgis, B. N. *Introduction to Ligand Fields*; Wiley: New York, 1966.
- (13) Frisch, M. J.; et al. *Gaussian03*, revision D.02; Gaussian, Inc.: Wallingford, CT, 2003.
- (14) Paul, F.; Toupet, L.; Thepot, J. Y.; Costuas, K.; Halet, J. F.; Lapinte, C. *Organometallics* **2005**, *24*, 5464.